Journal of Ceramic Processing Research. Vol. 14, No.2, pp. 226~229 (2013)

J O U R N A L O F
Ceramic Processing Research

Hydrothermal synthesis and gas-sensing property of SnO_2 nanorod clusters

Sitthisuntorn Supothina[a,*], Mantana Suwan[a] and Anurat Wisitsoraat[b]

[a]*National Metal and Materials Technology Center, 114 Thailand Science Park, Paholyothin Rd., Klong Luang, Pathumthani 12120, Thailand.*

[b]*National Electronics and Computer Technology Center, 112 Thailand Science Park, Paholyothin Rd., Klong Luang, Pathumthani 12120 Thailand*

SnO_2 were synthesized by hydrothermal treatment of colloidal hydrous tin oxide at 160-200 ºC for 48 hrs. The colloidal hydrous tin oxide precursor was prepared by mixing 0.188 M $Na_2SnO_3 \cdot 3H_2O$ solution with 0.35 M NaOH solution followed by the addition of absolute ethanol at ambient temperature under vigorous stirring until the white suspension was completely formed. XRD, SEM and TEM analyses revealed that SnO_2 clusters of 2.2 ± 0.15 μm in size consisting of tetragonal-shaped, single crystalline SnO_2 nanorods of 276 ± 30 nm wide and 1.33 ± 0.15 μm long was obtained at 200 ºC while SnO_2 nanoparticles of 228 ± 81 nm in size consisting of 6.9 ± 1.1 nm crystals were obtained at 160-180 ºC. Some single crystalline elongated particles of 224 ± 40 nm wide and 584 ± 126 nm long were also formed at 180 ºC. Gas-sensing study of the screen-printed SnO_2 nanorod sensor revealed that the sensor had good selectivity toward H_2S as it showed high response to 10 ppm H_2S, only moderate response to 10 ppm NO_2, and very low responses to 1000 ppm CO and 1000 ppm SO_2. The sensor showed good response to 0.3 ppm H_2S at relatively low operating temperature of 300 ºC with the response and recover times of ~ 1 and 3-4 minutes, respectively.

Key words: SnO_2, Nanorod, Hydrothermal, Gas sensor, Hydrogen sulfide.

Introduction

The recognition of gas-sensing capability of a semiconducting oxide in 1960s [1] has triggered the research in this field and led to the development of gas-sensing devices for inflammable and toxic gas detections. Among various semiconducting oxides, tin oxide (SnO_2) which is an n-type semiconductor with a wide band-gap of 3.6 eV has been recognized for its high sensitivity toward reducing gases [2-4]. However, the need for more accurate, low-concentration detection has driven the research for high-performance materials. During the past decade, nanostructured SnO_2 of various morphologies such as nanorod, nanowire, nanobelt, nanoflower and hollow sphere have been synthesized and studied for gas-sensing performance to gain benefit from their high surface-to-volume ratio [5-12]. The studies revealed that gas-sensing performance can be enhanced when the sensing material is in the form of nanostructure.

The nanostructured SnO_2 have been synthesized by several methods such as thermal evaporation [8], spray pyrolysis [9], hydrothermal/sovothermal [5, 6, 11, 13], as well as microemulsion [12]. The hydrothermal has been widely employed to synthesize the 1-dimensional nanostructures such as nanowire and nanorod because the anisotropic growth of the crystal can be favored under high pressure and temperature. In this study, SnO_2 nanorods were prepared by hydrothermal treatment of colloidal hydrous tin oxide at various temperatures, i.e., 160, 180 and 200 ºC, for 48 hrs. Gas sensing property was investigated toward H_2S, NO_2, CO and SO_2 over concentration ranges of 0.2-10, 0.2-10, 20-1000 and 20-1000 ppm, respectively.

*Corresponding author:
Tel : + (662) 564 6500
Fax: + (662) 564 6447
E-mail: sitthis@mtec.or.th (S. Supothina)

Experimental

The SnO_2 nanorods were synthesized by hydrothermal treatment of hydrous tin oxide prepared from precipitating reaction of sodium stannate trihydrate and sodium hydroxide following the method described elsewhere [13]. Briefly, 1.0 g $Na_2SnO_3 \cdot 3H_2O$ (Aldrich) was dissolved in 20 mL of 0.35 M NaOH (RCI Labscan) followed by dropwise addition of 20 mL of absolute ethanol (C_2H_5OH, RCI Labscan). The resulting solution was stirred for at least 30 min to obtain white suspension which was transferred into a 50-mL Teflon-lined stainless steel autoclave, and held in an electric oven at 200 ºC for 48 hrs. The product was thoroughly washed with deionized water, separated by vacuum filtration using a 0.1-μm cellulose membrane and finally dried at 105 ºC overnight. To study the effect of hydrothermal temperature on morphology of the product, the synthesis was also performed at 160 and 180 ºC.

Crystal structure of the sample was identified by using a JDX-3530 X-ray diffractometer (XRD, JEOL).

Morphology was observed by using a JSM-5410 scanning electron microscope (SEM, JEOL) and a JEM-2010 transmission electron microscope (TEM, JEOL).

Thick-film SnO_2 sensor was prepared as follow. An ethyl cellulose (Fluka, 30 - 70 mPa.s) temporary binder was dissolved in terpineol (Aldrich, 90%) solvent under stirring and heating at 80 °C. The solution was then mixed with an appropriate amount of SnO_2 nanorod powder and thoroughly ground for 30 min to form a paste. The resulting paste was screen printed on Al_2O_3 substrates (Semiconductor Wafer, Inc, 96%) interdigitated with Au electrodes (0.40 cm × 0.55 cm × 0.04 cm.) to form sensing film. An interdigit width, interdigit spacing and electrode area were 100 μm, 100 μm and 0.24 cm × 0.4 cm, respectively. The electrode pattern was fabricated by DC sputtering of 50 nm-thick Cr and 200 nm-thick Au layers and lift-off process. The resulting substrates were annealed in an oven at 150 °C for 1 hr and then at 400 °C for 1 hr with a heating rate of 1 °C/min for binder removal prior to the gas-sensing test.

Gas-sensing characteristics of the SnO_2 nanorod sensor were characterized toward H_2S, NO_2, CO and SO_2 over concentration ranges of 0.2-10, 0.2-10, 20-1000 and 20-1000 ppm, respectively. The standard flow through technique was used to measure the gas-sensing property. A constant flux of synthetic air of 2 L/min as gas carrier was mixed with the desired concentration of pollutants dispersed in synthetic air. All the measurements were conducted in a temperature-stabilized sealed chamber under controlled humidity. The gas flow rates were accurately manipulated using a computer controlled multi-channel mass flow controller. The external NiCr heater was heated by a regulated DC power supply to different operating temperatures ranging from 200 °C to 350 °C. The sensor resistance was continuously monitored using a voltage-amperometric technique with 1 V DC bias and current measurement through a picoammeter controlled by a computer. The sensor was exposed to a gas sample for 10 minutes at each gas concentration and the air flux was then restored for 25 minutes. The sensor response (S) is defined as the resistance ratio of R_a/R_g for reducing gas and R_g/R_a for oxidizing gas, where R_a is the resistance in dry air and R_g is the resistance in a reducing or oxidizing gas.

Results and discussion

Fig. 1 shows XRD patterns of the products prepared at 160, 180 and 200 °C. All the patterns are well matched with tetragonal SnO_2 (JCPDS# 41-1445). With the increased hydrothermal temperature, the patterns are sharper and have higher relative intensity indicating higher degree of crystallinity obtained from higher hydrothermal temperature. Relative intensities of the major planes are similar to those of standard

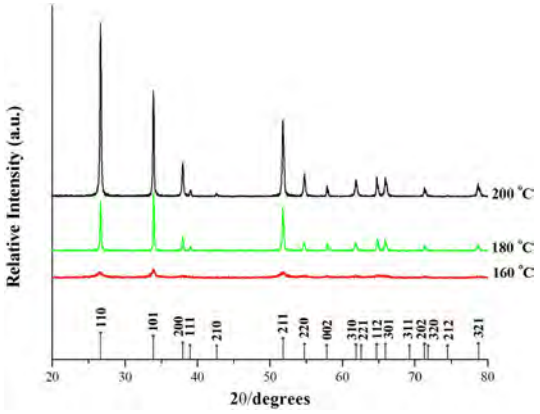

Fig. 1. XRD patterns of the products prepared at 160, 180 and 200 °C.

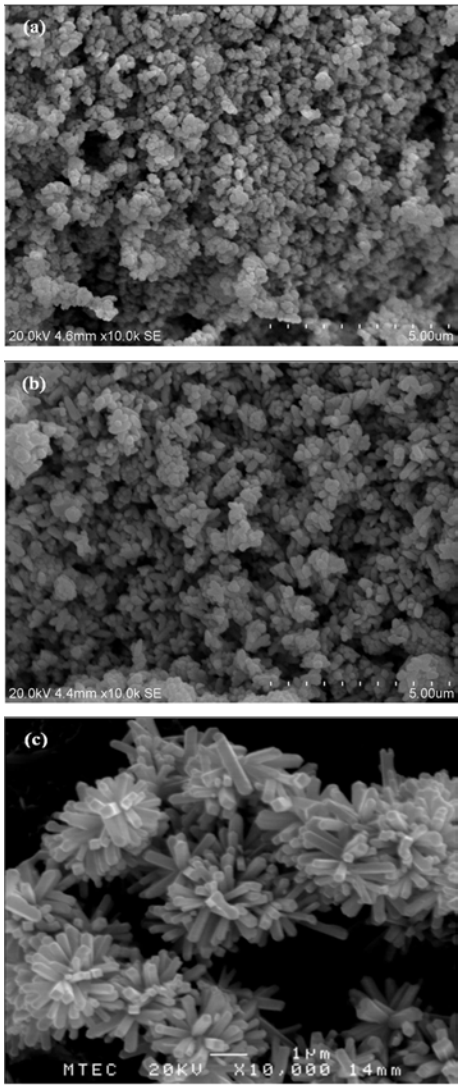

Fig. 2. SEM images of the products prepared at 160, 180 and 200 °C.

powder diffraction pattern, indicating that the products had no preferred orientation.

Fig. 2 shows SEM images of the SnO_2 prepared at 160, 180 and 200 °C. The morphology of the product is

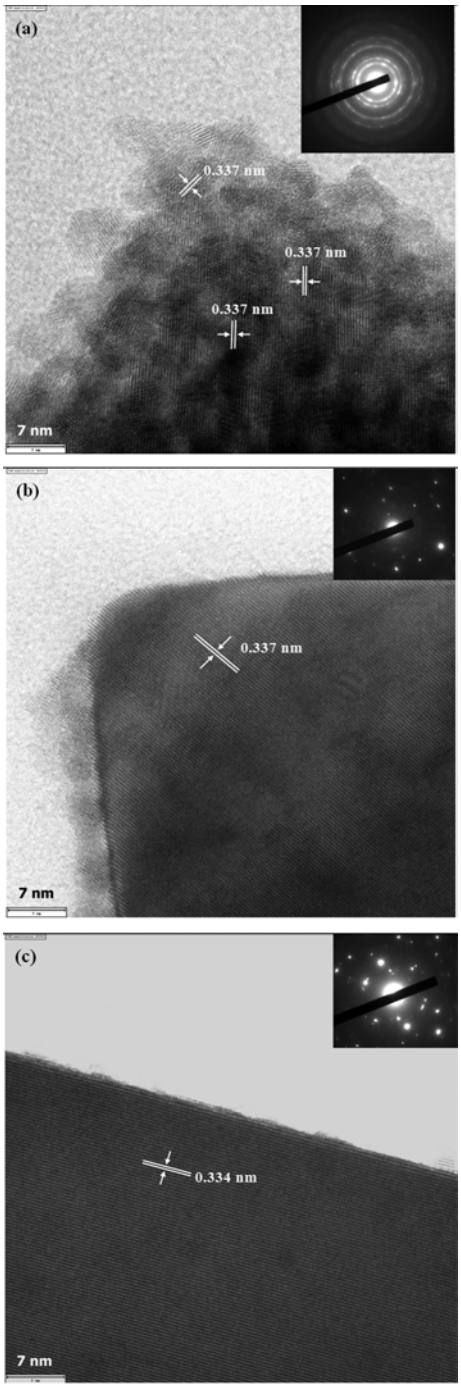

Fig. 3. TEM images of the products prepared at 160, 180 and 200 °C.

strongly dependent on the hydrothermal temperature. That is, at the synthesis temperature of 160 °C (Fig. 2(a)), the SnO_2 is observed as nanoparticles of 228 ± 81 nm as measured by an image analysis software. At 180 °C (Fig. 2(b)), nanoparticles of about the same size were obtained. However, some elongated particles of 224 ± 40 nm wide and 584 ± 126 nm long were also formed. When the hydrothermal was conducted at 200 °C, the product was tetragonal-shaped nanorods of 276 ± 30 nm wide and 1.33 ± 0.15 μm long aggregating homocentrically to form nanorod cluster of 2.2 ± 0.15 μm in size (Fig. 2(c)). In

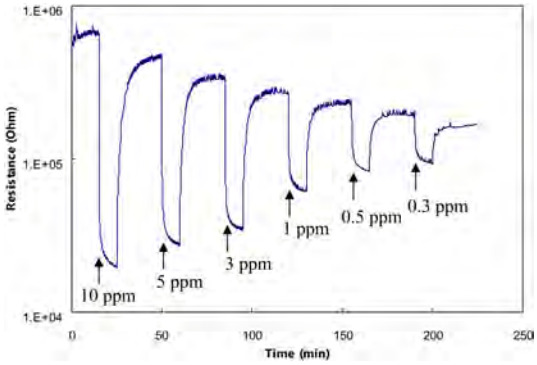

Fig. 4. Resistance change of SnO_2 nanorod sensor under exposure to various concentrations of H_2S ranging from 0.3 to 10 ppm at 300 °C.

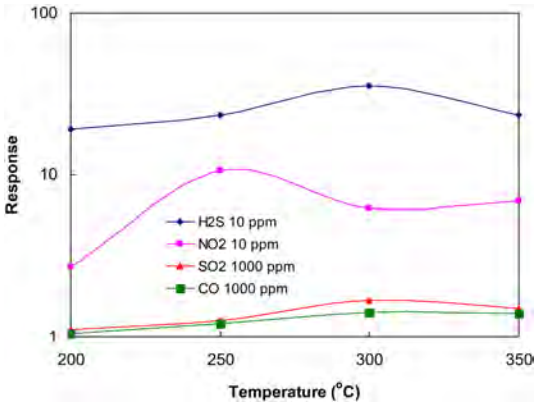

Fig. 5. Response of SnO_2 nanorod sensor versus operating temperature under exposure to 10 ppm H_2S, 10 ppm NO_2, 1000 ppm CO and 1000 ppm SO_2.

order to further investigate microstructure of the SnO_2 crystals, high-resolution TEM analysis was performed and the results shown in Fig. 3. The SnO_2 synthesized at 160 °C (Fig. 3(a)) is polycrystalline consisting of nanocrystals with uniform crystallite size of 6.9 ± 1.1 nm. A *d*-spacing of 3.37 Å matches well with that of the (110) plane of the tetragonal SnO_2 which is 3.35 Å (JCPDS# 41-1445 [14]) which is in good agreement with the XRD analysis. The selected-area electron diffraction pattern (SAED, inset) consists of sharp, discrete rings indicating polycrystalline structure. This result reveals that the nanoparticles observed under SEM (Fig. 2(a)) are polycrystalline. TEM investigation performed on the elongated particle synthesized at 180 °C revealed clear lattice fringes along the entire grain indicating single crystalline. Fig. 3(b) is a TEM image taken at the edge of the elongated grain. The *d*-spacing of 3.37 Å confirms the tetragonal SnO_2 phase. Its SAED pattern consists of sharp spots indicating single crystalline nature. Fig. 3(c) is a TEM image taken at the middle of the nanorod synthesized at 200 °C which is single crystalline with *d*-spacing of 3.34 Å which is slightly less than that of the nanoparticle and nanograin but very well matched with the standard tetragonal SnO_2.

Fig. 4 shows a typical resistance change of the SnO_2

nanorod sensing layer under exposure to various concentrations of H_2S ranging from 0.3 to 10 ppm at 300 °C. It can be seen that the resistances decrease drastically during the gas exposure with increasing gas concentration, which confirms a typical n-type semiconducting behavior towards reducing gas. As the H_2S gas concentration increases, the responses to H_2S are increased correspondingly while the response and recover times are in the same range of ~ 1 and 3-4 minutes, respectively. In addition, considerable downward baseline shift is observed after several H_2S exposure. Similar behaviors have been observed for other gases but the magnitudes of resistance changes are significantly different.

Fig. 5 shows the response of SnO_2 nanorod sensing layer versus operating temperature under exposure to 10 ppm H_2S, 10 ppm NO_2, 1000 ppm CO and 1000 ppm SO_2. It is evident that the SnO_2 nanorod cluster exhibits high, moderate, low and very low response to H_2S, NO_2, SO_2 and CO respectively. In addition, it has different optimal operating temperatures for different gases. The optimal operating temperature for H_2S, SO_2 and CO is around 300 °C while that for NO_2 is about 250 °C. The observed results are comparable with SnO_2 gas sensors fabricated by various synthetic methods such as flame spray pyrolysis [15-17], radio-frequency sputtering [18] and hydrolyzation [19]. Compared to these methods, hydrothermal synthesis presents some important advantages including low synthesis temperature, well controlled crystallite size and low cost. Thus, the SnO_2 nanorod cluster prepared by hydrothermal synthesis is a promising candidate for H_2S-sensing application.

Conclusions

SnO_2 nanorod clusters of 2.2 ± 0.15 μm in size consisting of tetragonal-shaped, single crystalline SnO_2 nanorods of 276 ± 30 nm wide and 1.33 ± 0.15 μm long was obtained by hydrothermal treatment of hydrous tin oxide suspension under basic condition at 200 °C for 48 h. The hydrothermal temperature had strong effect on morphology of the SnO_2 products. The nanorods can be synthsized at 200 °C whereas only nanoparticles of the same crystal structure were formed at lower temperatures. Based on the gas-sensing test against 10 ppm H_2S, 10 ppm NO_2, 1000 ppm CO and 1000 ppm SO_2, the screen-printed SnO_2 nanorod sensor was selective to H_2S. It showed high response to 0.3-10 ppm H_2S at relatively low operating temperature of 300 °C with the response and recover times of ~ 1 and 3-4 minutes, respectively.

Acknowledgments

The authors would like to acknowledge the National Metal and Materials Technology Center, Thailand, for financial support of this study (Grant# MT-B-52-CER-07-230-I).

References

1. T. Seiyama, A. Kato, K. Fujushi, and M. Nagatani, Anal. Chem. 34 (1962) 1502-1503.
2. W. Göpel, and K.D. Schierbaum, Sens. Actuators B: Chem. 26-27 (1995) 1-12.
3. N.S. Baik, G. Sakai, N. Miura, and N. Yamazoe, Sens. Actuators B: Chem. 63 (2000) 74-79.
4. T. Sahm, L. Mädler, A. Gurlo, N. Barsan, S.E. Pratsinis, and U. Weimar, Sens. Actuators B: Chem. 98 (2004) 148-153.
5. H. Wang, J. Liang, H. Fan, B. Xi, M. Zhang, S. Xiong, Y. Zhu, and Y. Qian, J. Solid State Chem. 181 (2008) 122-129.
6. X. Jiaqiang, W. Ding, Q. Lipeng, Y. Weijun, and P. Qingyi, Sens. Actuators B: Chem. 137 (2009) 490-495.
7. A. Biaggi-Labiosa, F. Solá, M. Lebrón-Colón, L.J. Evans, J.C. Xu, G.W. Hunter, G.M. Berger, and J.M. González, Nanotechnology 23 (2012) 455501-455508.
8. I.S. Hwang, S.J. Kim, J.K. Choi, J.J Jung, D.J. Yoo, K.Y. Dong, B.K. Ju, and J.H. Lee, Sens. Actuators B: Chem. 165 (2012) 97-103.
9. E. Brunet, T. Maier, G.C. Mutinati, S. Steinhauer, A. Köck, C. Gspan, and W. Grogger, Sens. Actuators B: Chem. 165 (2012) 110-118.
10. E. Comini, G. Faglia, G. Sberveglieri, D. Calestani, L. Zanotti, and M. Zha, Sens. Actuators B: Chem. 111-112 (2005) 2-6.
11. A.A. Firooz, A.R. Mahjoub, and A.A. Khodadadi, Sens. Actuators B: Chem. 141 (2009) 89-96.
12. F. Gyger, M. Hübner, C. Feldmann, N. Barsan, and U. Weimar, Chem. Mater. 22 (2010) 4821-4827.
13. S. Supothina, R. Rattanakam, S. Vichaphund, P. Thavorniti, J. Eur. Ceram. Soc. 31 (2011) 2453-2458.
14. Joint committee on Powder Diffraction Standards, Swarthmore, PA, PDF No. 41-1445.
15. T Sahm, L. Mädler, A. Gurlo, N. Barsan, S.E. Pratsinis, and U. Weimar, Sens. Actuators B: Chem. 98 (2004) 148-153.
16. L. Mädler, A. Roessler, S.E. Pratsinis, T. Sahm, A. Gurlo, N. Barsan, and U. Weimar, Sens. Actuators B: Chem. 114 (2005) 283-295.
17. C. Liewhiran, N. Tamaekong, A. Wisitsora-at, and S. Phanichphant, Sens. Actuators B: Chem. 163 (2012) 51-60.
18. A. Sharma, M. Tomar, and V. Gupta, Sens. Actuators B: Chem. 156 (2011) 743-752.
19. J. Zhang, S. Wang, Y. Wang, Y. Wang, B. Zhu, H. Xia, Z. Guo, S. Zhang, W. Huang, and S. Wu, Sens. Actuators B: Chem. 135 (2009) 610-617.